Double- and single-differential and total ionization cross sections for electron-impact ionization of a helium atom

R. Biswas and C. Sinha
Department of Theoretical Physics, Indian Association for the Cultivation of Science, Jadavpur, Calcutta 700 032, India
(Received 20 October 1995; revised manuscript received 14 February 1996)

Double, single, and total ionization cross sections have been calculated for the single ionization process of an electron-helium atom system for the incident energy range (50–300 eV) including the electron exchange effect. The final-state wave function involves a correlated three-body Coulomb continuum, and satisfies the three-body asymptotic boundary condition. The electron exchange effect is found to play a dominant role for near-symmetric and symmetric geometries. All results have been compared with available experiments, and reasonably good agreement has been noted except for low incident energies (e.g., 50 eV) and low ejected energies (in the double-differential or single-differential cross-section level). [S1050-2947(96)06609-7]

PACS number(s): 34.80.Dp

INTRODUCTION

In electron-impact ionization of atoms, cross sections for the production of low-energy secondary electrons ejected during ionization by fast electrons are of immense importance in plasma physics, atmospheric physics, and radiation physics. In particular, knowledge of angular and energy distributions is essential in radiation physics, since the secondary electrons produced along the paths of energetic charged particles are mainly responsible for the damage by radiation. Apart from this, the absolute total ionization cross sections has direct applications in fusion energy research and in astrophysics. The increasing availability of the experimental data for both the total and partial (differential) cross sections (e.g., triple, double, and single), have stimulated a significant amount of theoretical interest in the study of such cross sections. In particular, the helium atom, being one of the most preferred targets for the experimentalists (from a technical point of view) has been the subject of extensive theoretical investigation as well.

In the present work we have studied the double and single differential as well as the total ionization cross sections for single ionization of a helium atom by electron impact at intermediate and high incident energies. The double-differential cross sections (DDCS's) of the secondary ejected electron have been obtained by integrating the triple-differential cross sections (TDCS's) over the entire angular range of the primary (scattered) electron, while the single-differential cross section (SDCS) is obtained on integrating the DDCS over the entire angular range of the ejected electron. Further integration of the SDCS over the energy range of the ejected electron yields the integrated or total cross section.

The final-state wave function in the present model consists of a correlated three-body Coulomb continuum [Brauner, Briggs, and Klar (BBK) [1]], satisfying the asymptotic three-body boundary condition which is one of the most important criteria for obtaining reliable ionization cross sections. In this context it should be mentioned that the DDCS results for the electron–helium-atom system were also calculated earlier [2] by the present authors, where, unlike the BBK model, the two outgoing electrons were treated on unequal footing, and as such the final-state prescription was particularly appropriate for asymmetric geometry. The BBK model, on the other hand, is more versatile, and should be suitable for both symmetric (equal energy sharing) and asymmetric (unequal energy sharing) geometries. Since the ultimate goal of the present work is to determine the total ionization cross sections (TCS's) which cover both asymmetric and symmetric geometries, the BBK description is adopted here. However, the contribution of the latter geometry to the total ionization cross section is much smaller than that of the former one.

The two outgoing electrons in the final channel are considered to be indistinguishable, and hence the electron exchange effect has to be taken into account.

THEORY

The prior forms of direct and exchange matrix elements for the e^--He ionization process are given by

$$f=\langle \Psi_f^-(\vec{r}_1,\vec{r}_2,\vec{r}_3)|V_i|\psi_i(\vec{r}_1,\vec{r}_2,\vec{r}_3)\rangle \tag{1a}$$

and

$$g=\langle \Psi_f^-(\vec{r}_2,\vec{r}_1,\vec{r}_3)|V_i|\psi_i(\vec{r}_1,\vec{r}_2,\vec{r}_3)\rangle \tag{1b}$$

Since the choice of the simple uncorrelated Hylleraas wave function for the ground state of the He atom yielded reasonably good DDCS results before [2], the same has been used for the present calculations. This enables us to economize on the computation; particularly for the calculation of the SDCS and TCS. We thus choose

$$\phi_i(\vec{r}_2,\vec{r}_3)=u(\vec{r}_2)u(\vec{r}_3), \tag{2}$$

with

$$u(\vec{r})=[Z_t'^3/\pi]^{1/2}\exp(-Z_t'r)$$

Z_t' being the screened charge, $Z_t'=Z_t-\frac{5}{16}$.

The wave function $\phi(\vec{r}_2,\vec{r}_3)$ of the helium subsystem in

the final-channel is represented by a symmetrized product of the He^+ ground-state wave function (ϕ^+_{He}) for the bound electron with the continuum wave function $\phi_{\vec{k}_2}$ for the ejected electron with momentum $\vec{k}_2$ [orthogonalized to the ground-state orbital $u(\vec{r})$]. We write the final channel wave function Ψ_f^- in the following form:

$$\Psi_f^-(\vec{r}_1,\vec{r}_2,\vec{r}_3)=(2\pi)^{-3/2}\exp(-\tfrac{1}{2}\pi\alpha_1)\Gamma(1-i\alpha_1)\exp(i\vec{k}_1\cdot\vec{r}_1)\ {}_1F_1[i\alpha_1,1;-i(k_1r_1+\vec{k}_1\cdot\vec{r}_1)]\exp(-\tfrac{1}{2}\pi\alpha_{12})$$
$$\times\Gamma(1-\alpha_{12})\ {}_1F_1[i\alpha_{12},1;-i(k_{12}r_{12}+\vec{k}_{12}\cdot\vec{r}_{12})]\phi(\vec{r}_2,\vec{r}_3) \tag{3a}$$

with

$$\phi(\vec{r}_2,\vec{r}_3)=\frac{1}{\sqrt{2}}\,[\overline{\phi_{\vec{k}_2}}(\vec{r}_2)\,\phi_{He^+}(\vec{r}_3)+\overline{\phi_{\vec{k}_2}}(\vec{r}_3)\,\phi_{He^+}(\vec{r}_2)],$$

$$\overline{\phi_{\vec{k}_2}}(\vec{r})=\phi_{\vec{k}_2}(\vec{r})-\langle\phi_{\vec{k}_2}|u\rangle u(\vec{r}),$$

where

$$\phi_{\vec{k}_2}(\vec{r})=(2\pi)^{-3/2}\exp(-\tfrac{1}{2}\pi\alpha_2)\Gamma(1-i\alpha_2)$$
$$\times\exp(i\vec{k}_2\cdot\vec{r}_2)\ {}_1F_1[i\alpha_2,1;-i(\vec{k}_2\cdot\vec{r}_2+k_2r_2)],$$
$$\alpha_1=-Z_{sc}/k_1,\quad \alpha_2=-Z_{sc}/k_2,\quad \alpha_{12}=1/(2|\vec{k}_{12}|); \tag{3b}$$
$$\vec{k}_{12}=\tfrac{1}{2}(\vec{k}_1-\vec{k}_2),$$

Z_{sc} being the screened charge equal to 1. Equations (3a) and (3b) reveal that the final-state wave function Ψ_f^- that involves a correlated three-body Coulomb continuum satisfies the asymptotic (for r_1, r_2, $r_{12}\to\infty$) boundary condition [1,3]. Finally the expressions for the TDCS, DDCS, SDCS, and TCS, respectively, are given by (including the electron exchange effect in the final channel)

$$\frac{d^3\sigma}{d\Omega_1 d\Omega_2 dE_2}=(2\pi)^4\,\frac{k_1k_2}{k_i}\,[\tfrac{1}{4}|f+g|^2+\tfrac{3}{4}|f-g|^2], \tag{4}$$

$$\frac{d^2\sigma}{d\Omega_2 dE_2}=\int\left[\frac{d^3\sigma}{d\Omega_1 d\Omega_2 dE_2}\right]d\Omega_1, \tag{5}$$

$$\frac{d\sigma}{dE_2}=\int\left[\frac{d^2\sigma}{d\Omega_2 dE_2}\right]d\Omega_2, \tag{6}$$

$$\sigma=\int_0^{(E_i-\mathrm{IP})/2}\left[\frac{d\sigma}{dE_2}\right]dE_2, \tag{7}$$

where E_i is the incident energy and IP is the ionization potential of the helium atom. The evaluation of the ionization amplitudes (f and g) in Eq. (1) consists of two parts: (i) analytical and (ii) numerical. The first part has been carried out following our earlier method of calculation [4]. However, for the numerical part, we could not resort to our earlier numerical approach [4] because of the convergence difficulties arising during the numerical integrations. Thus for the present numerical evaluation we have adopted our recently developed technique [5], which is free from such difficulties. After analytical reduction, the amplitude f or g finally involves a two-dimensional integral which has been evaluated numerically.

RESULTS AND DISCUSSION

We have computed the DDCS and SDCS as well as the total ionization cross sections (TCS's) for single ionization of a helium atom by electron impact in the intermediate- and high-energy region (50–300 eV). The parameters have been chosen in accordance with the available experimental data. Figures 1–8 demonstrate the present DDCS results, our previous theoretical results of DDCS in a simpler (eikonal) model [2] as well as the experimental data of two different groups [6,7].

As may be noted from Figs. 1–8, the DDCS results of the two experimental groups [6,7] differ significantly with each other mainly quantitatively and sometimes qualitatively, particularly at low ejection angles. Figs. 1–6 demonstrate that at higher incident energies, e.g., at 300 and 200 eV, the physical features of the experimental DDCS's [6,7] are more or less well described by the present model, except at lower ejected angles, where the experiment due to Shyn and Sharp

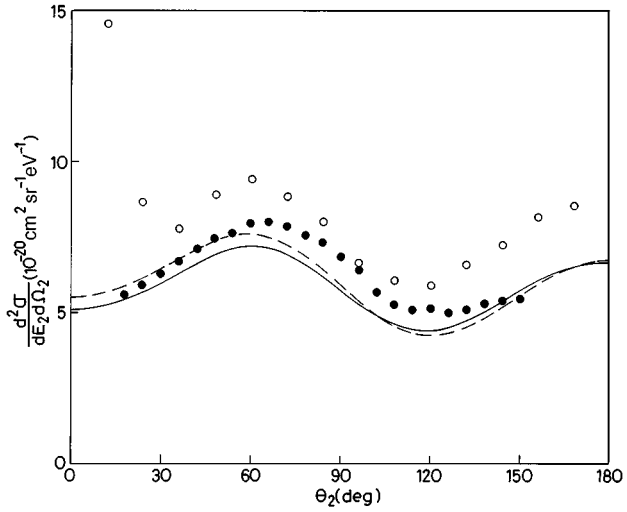

FIG. 1. The DDCS (in 10^{-20} cm^2 Sr^{-1} eV^{-1}) for electron-impact single ionization of helium from the ground state has been plotted as a function of the ejection angle θ_2 for incident energy (E_i)=300 eV and ejected energy (E_2)=10 eV. —, present results. — — — — —, theoretical results from eikonal model [2]. ●, experimental results of Müller-Fiedler, Jung, and Ehrhardt [7]. ○, experimental results of Shyn and Sharp [6].

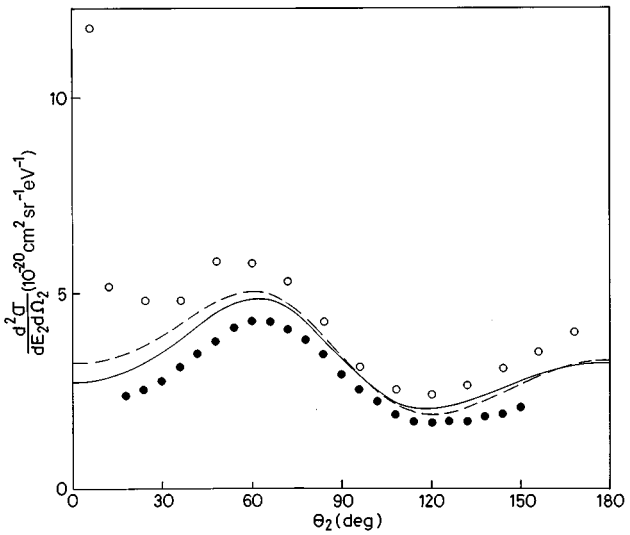

FIG. 2. Same as Fig. 1, but with E_2=20 eV.

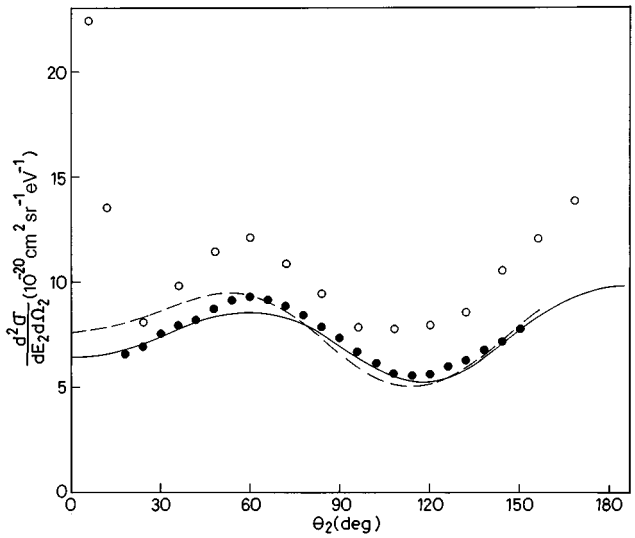

FIG. 4. Same as Fig. 1, but with E_i=200 eV.

[6] always shows a sharp rise at around (~6°) (Figs. 1–6). However, it should be pointed out that this particular feature in the results of Shyn and Sharp [6] is somewhat controversial in the sense that it has not shown up in any other DDCS experiments [7–9], nor is it present in other existing theories [2,10,11]. At the above-mentioned energies, the position of the present DDCS peak agrees quite well with the experiments [6,7]. However, quantitatively there is some discrepancy between the present DDCS and the measurements. To be specific, the overall agreement of the present DDCS with the experimental data of Müller-Feidler, Jung, and Ehrhardt [7] is good enough for the incident energy E_i=200 eV, while for higher incident energy E_i=300 eV (Figs. 1–3), the agreement is not so satisfactory. As for the comparison with the other experiment [6], it may be noted that (see Figs. 1 and 2 and 4 and 5) at lower E_2, the present DDCS underestimates the results of Shyn and Sharp [6], while for higher E_2 (Figs. 3 and 6), the situation is reversed qualitatively. However, in the latter case the quantitative agreement is much better than in the former. Particularly, for the kinematics E_i=300 eV and E_2=40 eV, (see Fig. 3) the present DDCS agrees well with the data of Shyn and Sharp [6].

Figures 7 and 8 demonstrate the present DDCS curves and our previous DDCS results [2], together with the corresponding experimental data [6,7] at a lower incident energy (100 eV). As may be noted from the figures, the agreement of the present DDCS with the experiments is not so satisfactory at this incident energy. For both ejected energies, e.g., 10 and 20 eV (Figs. 7 and 8), the present DDCS results underestimate the experimental data [6,7] by a significant amount, particularly at lower ejected angles. However, at higher ejected angles, the agreement is better, particularly with the experiment of Müller-Feidler, Jung, and Ehrhardt [7]. The disagreement of the present DDCS with the experiments [6,7] at low ejected energies is not very surprising, and may be attributed mainly to the inadequate description of the ejected electron wave function due to the neglect of short-range effects.

Regarding the comparison of the present DDCS with those in our simpler model [2], the following inferences may be drawn from Figs. 1–8. The DDCS results in the two mod-

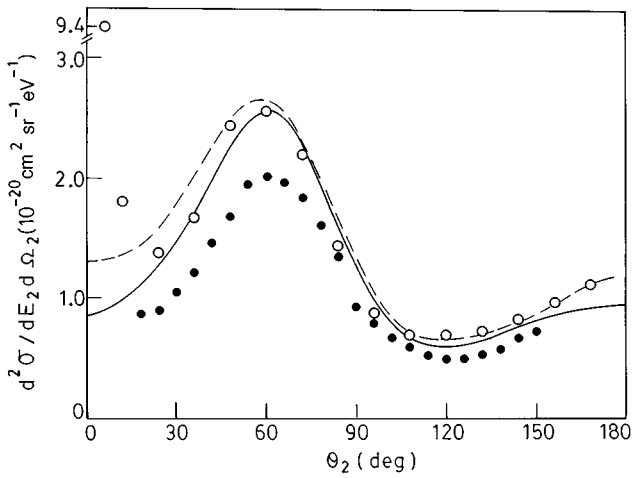

FIG. 3. Same as Fig. 1, but with E_2=40 eV.

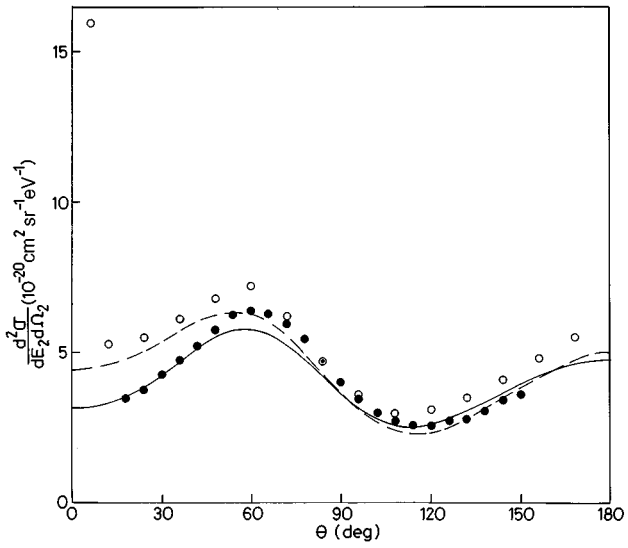

FIG. 5. Same as Fig. 4, but with E_2=20 eV.

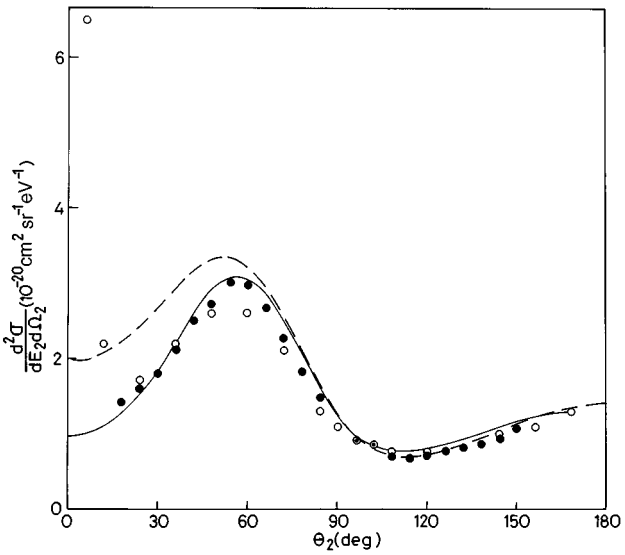

FIG. 6. Same as Fig. 4, but with E_2=40 eV.

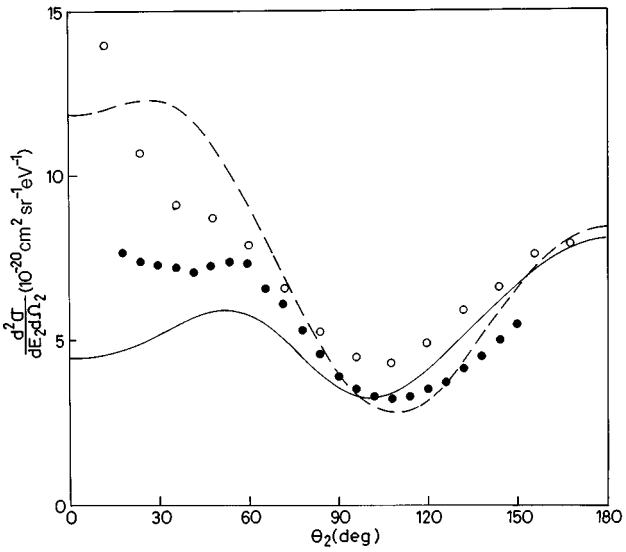

FIG. 8. Same as Fig. 7, but with E_2=20 eV.

els differ mainly at forward ejection angles (0°–90°), while the discrepancy diminishes in the backward direction (90°–180°). For forward ejection angles the eikonal DDCS lies above the corresponding BBK DDCS, they intersect at a particular ejection angle and, afterwards, with increasing ejection angle the eikonal curve lies slightly below the BBK curve. However, there is an exception to this behavior in Fig. 3 for the dynamics E_i=300 eV and E_2=40 eV. From the mathematical point of view the two models are equivalent asymptotically for asymmetric geometry (i.e., for $k_1 \gg k_2$). Physically, the basic difference between the two models lies in the fact that in the simpler eikonal model [2] the two outgoing electrons are treated on unequal footing, and this model is particularly suitable for asymmetric geometry, while the present model (BBK), in which the two emergent electrons are considered on an identical footing, covers both symmetric and asymmetric geometries and as such is more versatile. Thus for high incident energy and highly asymmetric collisions, the two models are expected to give similar results, but as the asymmetry decreases (i.e., with decreasing $|\vec{k}_1-\vec{k}_2|$), the BBK prescription should become more valid than the eikonal one (see Figs. 3 and 6). In fact for those dynamics where the Coulomb normalization constant (present in the BBK form only) plays a dominant role in determining some particular physical features in the DDCS or TDCS cross sections, the difference between the two models becomes appreciable. For instance, in the exact symmetry region, i.e., when $\vec{k}_1=\vec{k}_2$, the Coulomb normalization constant involving the correlation term [see Eq. (3a)] becomes zero for high repulsion between the two electrons, and therefore the cross sections vanish there. However, since the eikonal wave function does not involve the Coulomb normalization constant, it does not take account of this vanishing of the cross section and hence is not at all appropriate for the symmetric geometry. Further, for low incident energy, the BBK prescription should give a better result than the eikonal one since the latter is basically a high-energy approximation. This is quite apparent from Figs. 7 and 8 (for E_i=100 eV).

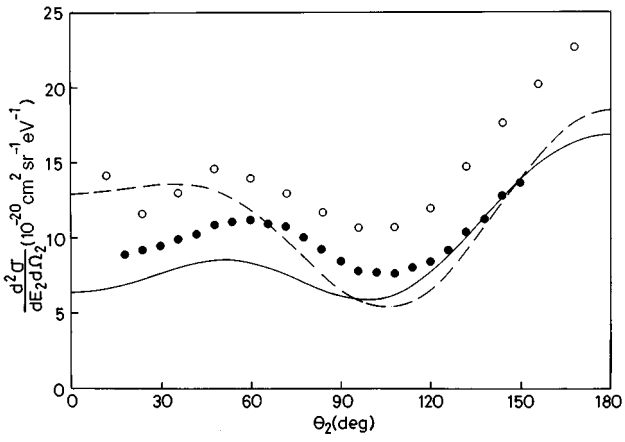

FIG. 7. Same as Fig. 1, but with E_i=100 eV.

Since the two measurements [6,7] for DDCS differ appreciably from each other, it is difficult to draw a definite conclusion regarding the agreement of the DDCS results from the two models with the experiments. However, keeping in mind the inconsistency between the two experiments [6,7], it may be inferred from Figs. 1–8 that, in general, for highly asymmetric collisions and high incident energy (e.g., E_i=300 eV and E_2=10 eV, Fig. 1), the eikonal cross section seems to be better than the BBK one, particularly for low ejection angles where the two theories disagree most. On the other hand, for a less asymmetric collision (e.g., E_i=200 eV and E_2=40 eV, Fig. 6), the BBK results appear to give better a agreement with the experiments. However, for a more rigorous comparison between the two models, we have to await a more refined experiment on the DDCS, where the ambiguity between different experimental results is expected to be removed.

Figures 9–11 exhibit the present single-differential cross sections (SDCS's) together with the existing experimental data [6,7,12,13] as well as other available theoretical SDCS results [11,14] for three incident energies 200, 100, and 50 eV, respectively. Figure 9 reveals that [E_i=200 eV] for lower ejected energies (E_2) the present SDCS is closer to the experimental data of Shyn and Sharp [6] than those of the

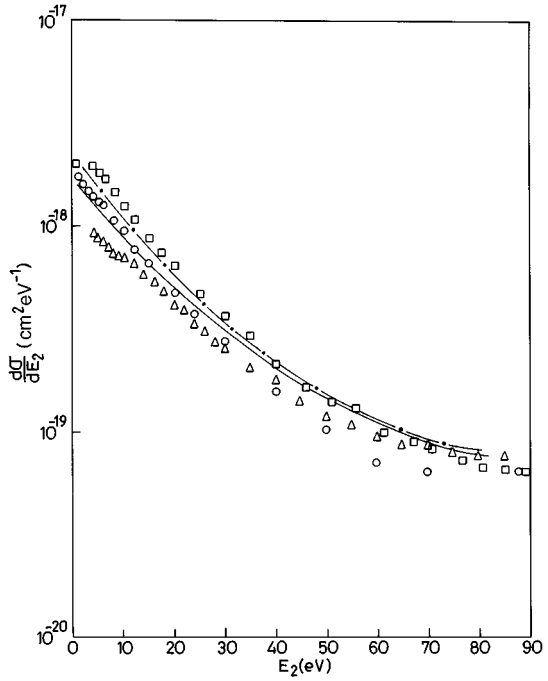

FIG. 9. The SDCS (in cm^2 eV^{-1}) for electron-impact single ionization of helium from the ground state has been plotted as a function of the ejection energy E_2 for incident energy (E_i)=200 eV. —, present results; –·–, results of Bransden, Smith, and Winters [11]. ○, experimental results of Shyn and Sharp [6]; □, experimental results of Opal, Beaty, and Peterson [12]; △, experimental results of Rudd and DuBois [13].

other two experiments [12,13], while for higher E_2 the situation is reversed.

Regarding the comparison with the other theoretical results of Bransden, Smith, and Winters [11] (see Figs. 9 and 10), the present SDCS curves are always found to lie below their curves for all values of E_2. However, the quantitative agreement between the two results is much better at 200 eV (Fig. 9) than at 100 eV (Fig. 10).

At 100 eV (see Fig. 10) the present SDCS results compare well with the measurements of Rudd and DuBois [13] and Opal, Beaty, and Peterson [12], as well as with the theoretical close-coupling (CC) results [14] except for lower ejected energies (E_2). In fact for low E_2, the CC results are in excellent agreement with the experimental data [12,13]. However, discrepancies between the present SDCS results and the experiment, as well as with the CC results for low E_2, are not unexpected, as discussed earlier in the context of DDCS results.

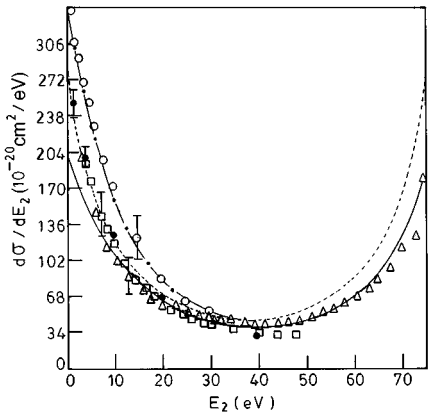

FIG. 10. Same as Fig. 9 but in 10^{-20}-cm^2 eV^{-1} units and for E_i=100 eV. – – – – – – –, results of Bray and Fursa [14]. ●, experimental results of Müller-Fiedler, Jung, and Ehrhardt [7].

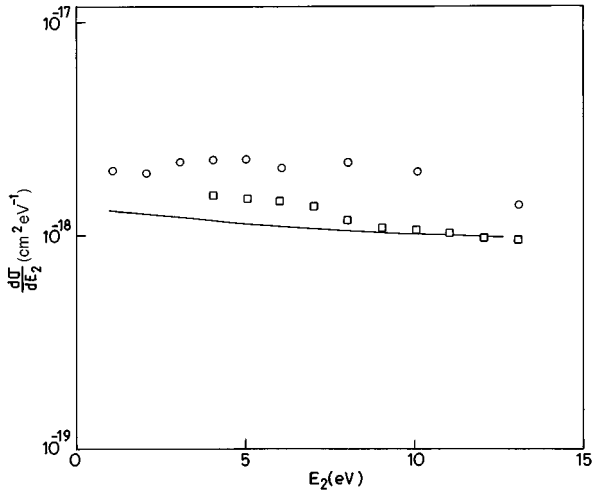

FIG. 11. Same as Fig. 9, but with E_i=50 eV.

As for the comparison with the other experiment [6], it may be inferred (see Fig. 10) that only the theoretical results of Bransden, Smith, and Winters [11] are in good agreement with the data of Shyn and Sharp [6], while the present results as well as the CC results are far from it, particularly at lower E_2. However, it should be mentioned here that the experimental data of Shyn and Sharp [6] at E_i=100 eV are not consistent with the other measurements [6,7,12,13] for low E_2, e.g., from 0 to 20 eV.

Figure 11 exhibits a comparison between the present SDCS and the two measurements [6,12] for the incident energy 50 eV. As is expected following our earlier discussions, the present results differ appreciably from both the experi-

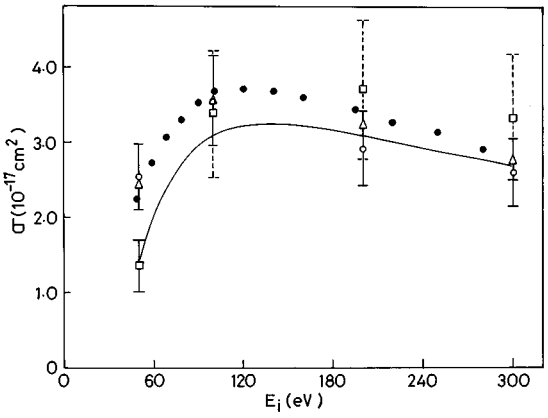

FIG. 12. The TCS (in 10^{-17} cm^2) for electron-impact single ionization of helium from the ground state has been plotted as a function of the incident energy E_i. —, present result. ●, experimental results of Shah *et al.* [16]; □, experimental results of Opal, Beaty and Peterson [12]; △, experimental results of Smith [15], ○, experimental results of Shyn and Sharp [6].

TABLE I. The following table shows numerical data for total single ionization cross sections σ (in 10^{-17}-cm^2 units) for electron-impact ionization of a helium atom for different incident energies from 50 to 300 eV, along with some experimental results [6,12,13,15,16,17] available in the literature.

	Total ionization cross sections σ in units of 10^{-17} cm^2						
Incident energy E_i in eV	Smith [15]	Opal Beaty, and Peterson [12]	Rudd and DuBois [13]	Shyn and Sharp [6]	Montague, Harrison, and Smith [17]	Shah *et al.* [16]	Present result
50	2.44	1.36 ±0.34		2.54 ±0.43	2.30		1.39
75					3.21		2.62
100	3.54	3.37 ±0.84	2.96 ±0.74	3.54 ±0.60	3.58	3.67 ±0.08	3.08
150					3.62	3.60 ±0.04	3.23
200	3.22	3.67 ±0.92	2.34 ±0.59	2.90 ±0.49	3.39		3.07
250					3.12	3.13 ±0.04	2.87
300	2.74	3.31 ±0.83		2.58 ±0.44	2.88		2.66

ments [6,12] for low E_2. However, with increasing E_2 it become closer to the measurements of Opal, Beaty, and Peterson [12].

It may be mentioned in the context of the SDCS study that the electron exchange effect is found to be appreciably high for the near-symmetric and symmetric kinematics, particularly at low incident energies. In fact in some specific cases (e.g., at E_i=100 eV) the exchange cross sections (DDCS's) are sometimes (for equal sharing) higher than the direct cross sections by even an order of magnitude.

Finally, the last figure (Fig. 12) depicts the total single-ionization cross section (TCS) for the incident energies 50–300 eV. The qualitative nature of the present TCS curve more or less agrees with all the experimental results [6,12,15,16]. Quantitatively, the present curve lies well within the experimental errors of all the experiments [6,12,15], barring the results of Shah *et al.* [16], for which the present curve always underestimates. In fact the TCS results of Shah *et al.* [16] lie well above all the other experimental data [6,12,15].

Table I provides a quantitative comparison between the present TCS and the corresponding different experimental data [6,12,15–17] for the incident energy range 50–300 eV. As may be noted from Table I, the present model adequately describes the total ionization cross sections when compared with the experiments [6,12,15,16,17] except at low incident energies (e.g., 50 eV). The agreement is better with increasing incident energy, as is expected.

CONCLUSION

We would like to comment that, since the calculation of TCS's involve all types of geometries (symmetric as well as asymmetric) one should adopt the more versatile prescription (BBK) for the sake of consistency. However, by virtue of the fact that the contribution of the symmetric geometry to the TCS is much smaller than that of the asymmetric one (as is also reflected from the SDCS curves, Figs. 9 and 10), the simpler model (eikonal) is also expected to give a reasonable estimate of the total ionization cross sections (TCS's).

For lower ejected energy (E_2), the discrepancy between both the DDCS results (from the two models) and the experiments may mainly be attributed to the inadequate description of the ejected electron wave function due to the neglect of short-range forces in both models. Thus, to improve the differential as well as the total cross section results, one should consider the short-range effects, particularly in the description of the ejected electron wave function. Further, distortion in the incident wave as well as a better prescription of the bound-state He-atom wave function might also add to the improvement of the results in both models.

[1] M. Brauner, J. S. Briggs, and H. Klar, J. Phys. B **22**, 2265 (1989).
[2] R. Biswas and C. Sinha, Phys. Rev. A **51**, 3766 (1995).
[3] M. Brauner, J. S. Briggs, and J. T. Broad, J. Phys. B **24**, 287 (1991).
[4] C. Sinha and N. C. Sil, J. Phys. B **12**, 1711 (1978).
[5] R. Biswas and C. Sinha, Nuovo Cimento **16D**, 571 (1994).
[6] T. W. Shyn and W. E. Sharp, Phys. Rev. A **19**, 557 (1979).
[7] R. Müller-Fiedler, K. Jung, and H. Ehrhardt, J. Phys. B **19**, 1211 (1986).
[8] R. R. Goruganthu and R. A. Bonham, Phys. Rev. A **34**, 103 (1986).
[9] L. Avaldi, R. Camilloni, E. Fainelli, and G. Stefani, Nuovo Cimento **9D**, 97 (1987).

[10] K. L. Bell and A. E. Kingston, J. Phys. B **8**, 2666 (1975).
[11] B. H. Bransden, J. J. Smith, and K. H. Winters, J. Phys. B **12**, 1267 (1979).
[12] C. B. Opal, E. C. Beaty, and W. K. Peterson, At. Data **4**, 209 (1972).
[13] M. E. Rudd and R. D. DuBois, Phys. Rev. A **16**, 26 (1977).
[14] I. Bray and D. V. Fursa, J. Phys. B **28**, L435 (1995).
[15] P. T. Smith, Phys. Rev. **36**, 1293 (1930).
[16] M. B. Shah, D. S. Elliott, P. McCallion, and H. B. Gilbody, J. Phys. B **21**, 2751 (1988).
[17] R. G. Montague, M. F. A. Harrison, and A. C. H. Smith, J. Phys. B **17**, 3295 (1984).